nature structural & molecular biology

Dicer associates with chromatin to repress genome activity in *Schizosaccharomyces pombe*

Katrina J Woolcock, Dimos Gaidatzis, Tanel Punga & Marc Bühler

In the fission yeast *S. pombe*, the RNA interference (RNAi) pathway is required to generate small interfering RNAs (siRNAs) that mediate heterochromatic silencing of centromeric repeats. Here, we demonstrate that RNAi also functions to repress genomic elements other than constitutive heterochromatin. Using DNA adenine methyltransferase identification (DamID), we show that the RNAi proteins Dcr1 and Rdp1 physically associate with some euchromatic genes, noncoding RNA genes and retrotransposon long terminal repeats, and that this association is independent of the Clr4 histone methyltransferase. Physical association of RNAi with chromatin is sufficient to trigger a silencing response but not to assemble heterochromatin. The mode of silencing at the newly identified RNAi targets is consistent with a co-transcriptional gene silencing model, as proposed earlier, and functions with trace amounts of siRNAs. We anticipate that similar mechanisms could also be operational in other eukaryotes.

S. pombe contains single genes encoding the RNAi proteins Argonaute, Dicer and RNA-dependent RNA polymerase (*ago1*$^+$, *dcr1*$^+$ and *rdp1*$^+$, respectively). Deletion of any of these genes results in loss of heterochromatic gene silencing, markedly reduced levels of histone H3 Lys9 (H3K9) methylation (H3K9me) at centromeric repeat regions, and defects in chromosome segregation[1,2]. *S. pombe* expresses endogenous siRNAs, most of which correspond to heterochromatic regions and are found single stranded in an Ago1-containing complex, called the RNA-induced transcriptional silencing complex (RITS; consisting of Ago1, Chp1 and Tas3)[3,4]. Current models for RNAi-mediated heterochromatin formation in *S. pombe* propose that noncoding transcripts from repetitive elements are processed by Dcr1 into siRNAs, which guide the RITS complex to chromatin via complementary base-pairing of the Ago1-bound siRNA with the nascent RNA[4,5]. Subsequently this leads to recruitment of CLRC, a protein complex that contains the sole *S. pombe* H3K9 methyltransferase Clr4 (ref. 6). H3K9me further stabilizes binding of RITS to chromatin via its subunit Chp1 and provides binding sites for the heterochromatin proteins Swi6 and Chp2. RITS can also recruit the RNA-directed RNA polymerase complex (RDRC; consisting of Rdp1, Cid12 and Hrr1), generating more double-stranded RNA substrates for Dcr1 and amplifying the process[7,8]. Notably, it is assumed that this entire process occurs *in cis* on chromatin. This is directly supported by chromatin immunoprecipitation (ChIP) experiments that demonstrate a physical association of Ago1 and Rdp1 with chromatin[1,9]. However, attempts to cross-link Dcr1 to centromeric heterochromatin have failed[1]. Therefore, definitive proof for the *cis* model has been lacking, and the available data do not allow us to rule out the possibility that siRNA processing could occur off chromatin[10].

Although siRNAs are essential for proper heterochromatin assembly at centromeric repeats, they function poorly in *de novo* formation of heterochromatin at ectopic sites[5,11–13]. Furthermore, the accumulation of siRNAs and the methylation of H3K9 are mutually dependent processes in *S. pombe*, and the physical association of Ago1 with chromatin is lost in Clr4-deficient cells[7,9,14,15]. Notably, low levels of H3K9me persist at centromeres in RNAi-deficient cells, and genetic and biochemical analysis of the requirements for establishment and maintenance of centromeric heterochromatin have provided evidence that low levels of H3K9me play a crucial role in the initial steps of heterochromatin formation[1,16,17]. It has therefore been proposed that a siRNA-independent mechanism provides some low levels of H3K9me at centromeric repeats to allow the initial recruitment of the RNAi machinery to centromeres. This would then trigger a positive feedback loop to promote more efficient Clr4 recruitment and thus high levels of H3K9me and siRNAs[18]. How Clr4 is initially recruited to centromeres is debated. This process could be mediated by Dcr1-independent small RNAs, as recently proposed[19]. Alternatively, Clr4 might also be recruited via yet-to-be-identified *cis*-acting nucleation sites, as has been demonstrated for other heterochromatic loci in *S. pombe*[20].

In addition to its role in heterochromatin formation at centromeric repeats, the RNAi pathway has recently been implicated in the transient recruitment of the HP1 homolog Swi6 to some convergent gene pairs (CGPs)[21]. It is proposed that inefficient transcription termination at the studied CGPs leads to overlapping transcription in the G1 phase of the cell cycle, creating a double-stranded substrate for Dcr1. The resulting siRNAs would then target the RITS complex to the intergenic region, leading to H3K9 methylation and Swi6 binding. Swi6 in turn recruits cohesin, which ensures proper transcription termination for the remainder of the cell cycle. So far, this mechanism has been demonstrated only for a few gene pairs, and it remains unclear how widespread it is among CGPs across the whole *S. pombe* genome.

Here, we use DamID to probe the fission yeast genome for interactions with RNAi and heterochromatin proteins in a cell cycle–independent

Friedrich Miescher Institute for Biomedical Research, Basel, Switzerland. Correspondence should be addressed to M.B. (marc.buehler@fmi.ch).

Received 28 April; accepted 20 September; published online 12 December 2010; doi:10.1038/nsmb.1935

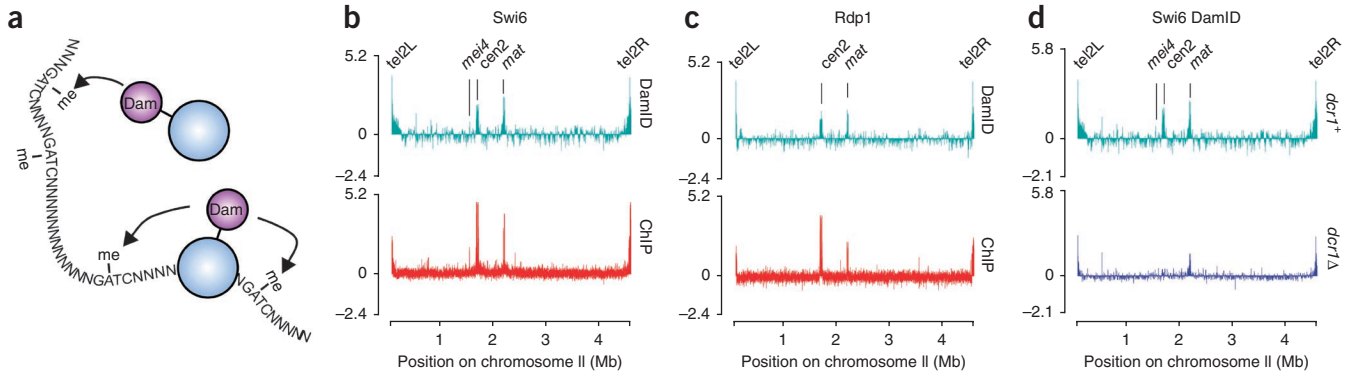

Figure 1 Identification of previously known and novel Swi6 and Rdp1 binding sites by DamID. (**a**) In DamID, a fusion protein consisting of a protein of interest and DNA adenine methyltransferase (Dam) from *Escherichia coli* is expressed at very low levels. On interaction of the fusion protein with chromatin, Dam methylates the N^6 position of adenine in the sequence context GATC. Thus, Dam leaves G^6mATC marks close to the genomic binding sites, which can be mapped by a methylation-specific PCR protocol (**Supplementary Fig. 1**). (**b**,**c**) Swi6 and Rdp1 maps for chromosome II as determined by DamID or ChIP-on-chip. (**d**) DamID map of Swi6 interactions for chromosome II in wild-type and *dcr1Δ* cells. For the DamID maps, the signal was averaged over every 500 probes. *y* axes are on $\log_2$ scale; *x* axes indicate position on chromosome II.

manner. We demonstrate that Swi6 can be recruited to a few but not all CGPs via the RNAi pathway, and we show for the first time that Dcr1 physically associates with chromatin, providing direct evidence for RNAi-mediated heterochromatin formation *in cis* at centromeric repeats. Unexpectedly, in the absence of H3K9 methylation, Dcr1, and to a certain extent Rdp1, can still associate with chromatin. On the basis of our results we propose that pre-existing H3K9 methylation is dispensable for siRNA generation, but not for proper loading of siRNAs onto Ago1, a process that ensures high levels of siRNAs and robust H3K9 methylation at centromeric repeats. In the absence of H3K9 methylation, Rdp1 and Dcr1 can still function on chromatin to trigger RNA decay but fail to accumulate high levels of siRNAs, a silencing mode that is consistent with a co-transcriptional gene silencing (CTGS) model, as proposed earlier[5,22].

RESULTS

Interactions of Swi6 and Rdp1 with the *S. pombe* genome

Previous genome-wide studies of RNAi-dependent heterochromatin formation in *S. pombe* have mainly used the ChIP technique to map interactions of proteins with chromatin[9,23], and deep sequencing technologies to identify sites of siRNA production[19,24,25]. Notably, *S. pombe* has an extended G2 phase, and as many of these studies used asynchronous cultures, they could have missed the association of proteins with chromatin or the production of small RNAs outside G2. Furthermore, attempts to immunoprecipitate certain components of the pathway with heterochromatin have failed[1,26], perhaps owing to insufficient sensitivity of the ChIP technique to detect indirect or weak interactions of proteins with chromatin. Similarly, even deep sequencing may be unable to detect small RNAs of very low abundance or stability. To address these problems, we took advantage of DamID[27], a highly sensitive chromatin profiling technique that is well suited to capture even transient protein-chromatin interactions that might occur during the cell cycle (**Fig. 1a** and **Supplementary Fig. 1**).

We first tested Swi6 and Rdp1, two proteins that are fully functional when fused to Dam (**Supplementary Fig. 2**) and for which genome-wide chromatin association profiles have been determined using ChIP in combination with microarrays (ChIP-on-chip)[9]. We hybridized samples from three independent DamID experiments to *S. pombe* tiling arrays from Affymetrix. A first analysis of the data revealed that DamID is a reliable method to detect both stable and transient Swi6 associations with the *S. pombe* genome (**Fig. 1** and data not shown). Comparing our data with the ChIP-on-chip data showed that DamID revealed all known major heterochromatic sites as well as their association with Rdp1 (**Fig. 1b**,**c**). As expected, Dcr1 was only partially required for Swi6 association with subtelomeric regions (as assessed by pseudogenes, most of which are located in subtelomeres) and the mating type locus, whereas Swi6 association with centromeric repeats was greatly affected in *dcr1Δ* cells (**Fig. 1d** and **Supplementary Fig. 3**). To investigate whether the DamID approach reveals so-far-unknown heterochromatic regions, we looked for regions that were enriched in the DamID but not in the ChIP-on-chip data and that were not located near known heterochromatic regions (**Supplementary Table 1**). This revealed a list of 28 elements for Swi6 and 11 elements for Rdp1 (**Supplementary Tables 2** and **3**). Notably, most of the newly identified Swi6-associated loci seem to be dependent on Dcr1, and many are part of a CGP and/or found near a noncoding RNA (ncRNA) gene.

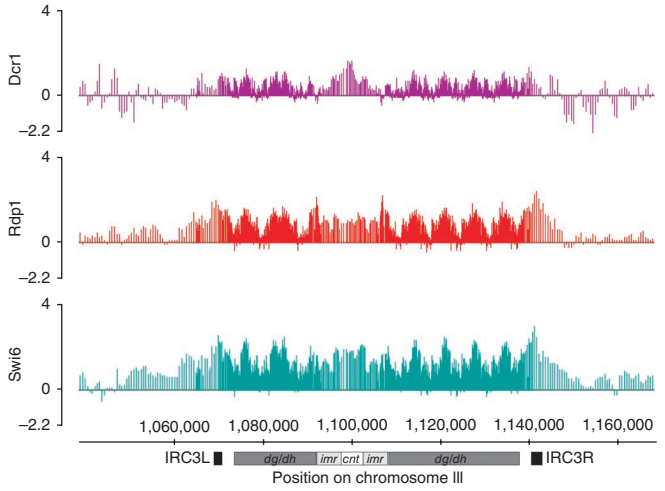

Figure 2 Dcr1 physically associates with centromeric chromatin. Dcr1, Rdp1 and Swi6 DamID maps for the centromeric region of chromosome III with flanking internal repeat elements (IRC3L/R), outermost repeats (*dg*/*dh*), innermost repeats (*imr*) and central core domain (*cnt*). The signal was averaged over every 50 probes. *y* axes are on $\log_2$ scale; *x* axes indicate position on chromosome III.

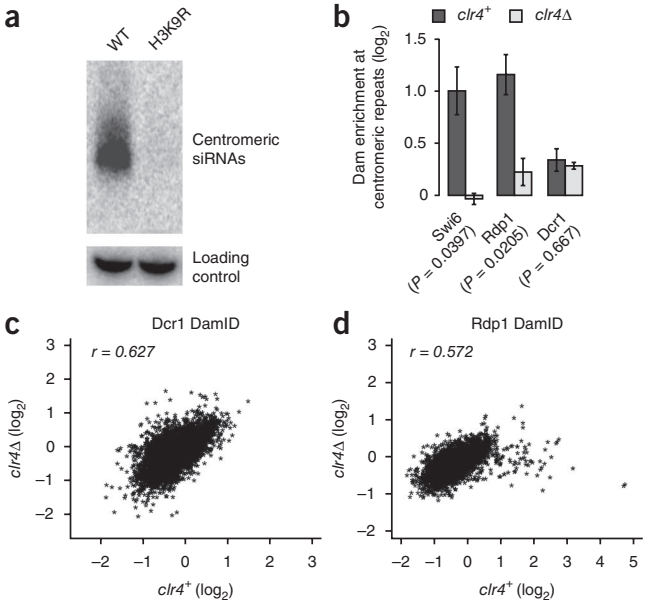

Figure 3 Clr4 dependency of Dcr1 or Rdp1 association with chromatin. (**a**) Northern blot for centromeric siRNAs in wild-type and heterochromatin-defective (H3K9R) cells. snoR69 serves as a loading control. (**b**) Swi6, Rdp1 and Dcr1 enrichment at centromeric repeat elements in wild-type and heterochromatin-defective (*clr4*Δ) cells. Error bars represent the s.e.m. ($n = 3$). *P* values were generated using the Student's *t*-test. (**c**,**d**) Comparisons of DamID signal quantified at annotated features across the genome in wild-type and heterochromatin-defective (*clr4*Δ) cells. Each axis shows the average of three independent biological replicates. (**c**) Dcr1 association is Clr4-independent across the whole genome. (**d**) Rdp1 association depends on Clr4 at some loci but not at others.

Dcr1 associates with chromatin independently of Clr4

A major advantage of using DamID is that it allows the detection of indirect protein-chromatin associations[28]. ChIP is inefficient in detecting interactions of proteins that do not bind to chromatin directly but rather bind via other proteins or chromatin-associated RNAs. For example, an association of Dcr1 with pericentromeric heterochromatin has so far not been demonstrated by ChIP[1], although current models propose that Dcr1 generates siRNAs *in cis* on centromeric chromatin[29]. We therefore set out to test whether Dam–Dcr1 would reveal any association with chromatin. Indeed, Dcr1 was revealed to be associated with centromeric repeats (**Fig. 2**), providing the first direct evidence that the entire RNAi machinery operates *in cis* to promote the assembly of centromeric heterochromatin.

An intriguing feature of the *S. pombe* RNAi pathway is that Clr4 is necessary for the accumulation of high siRNA levels. Consistent with previous studies[5,14,15,19], centromeric siRNA levels were drastically reduced when H3K9 methylation was prevented by either deleting *clr4*$^+$ or mutating H3K9 to H3R9 (**Fig. 3a** and data not shown), suggesting that Dcr1 might be recruited to centromeric repeats in a heterochromatin-dependent manner to generate siRNAs. DamID allowed us to test this model directly by comparing Dcr1 profiles in wild-type and *clr4Δ* cells. Unexpectedly, we found that Dcr1 still associated with centromeric repeats in *clr4Δ* cells (**Fig. 3b**). Notably, this pattern of Clr4 independence is seen throughout the genome for Dcr1 (**Fig. 3c**). Moreover, Rdp1 binding to centromeric repeats was significantly ($P = 0.0205$) reduced but not completely lost in *clr4Δ* cells (**Fig. 3b**,**d**). Therefore, the low centromeric siRNA levels observed in heterochromatin-deficient cells cannot be explained by the absence of the siRNA-processing machinery at centromeric repeats.

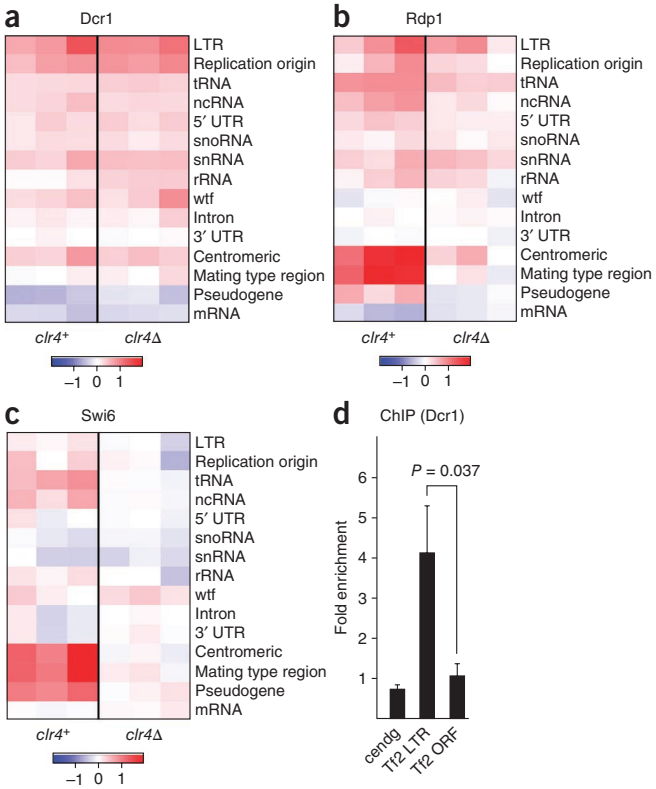

RNAi machinery contributes to long terminal repeat silencing

Having shown that Dcr1 directly associates with its known targets, we looked for other putative Dcr1-associated loci and found that it also associates with some euchromatic regions, including ncRNA genes and long terminal repeats (LTRs) (**Fig. 4a**). In total, we found 128 elements to be associated with Dcr1, 53 of them LTRs and 30 of them ncRNA genes (**Supplementary Table 4**). There are 13 full-length copies of the Tf2 LTR retrotransposon in the *S. pombe* genome, and ~250 solo LTRs or LTR fragments[30]. Using only unique probes and extending the LTR sequences by 200 bp on either side showed that ~65% of LTRs are associated with Dcr1. Unlike for centromeric repeats, we were able to confirm Dcr1 association with LTRs by ChIP (**Fig. 4**), suggesting that Dcr1 is more tightly associated with LTRs than centromeric repeat DNA.

Similar to what we saw for Dcr1, we also found Rdp1 to be associated with LTRs (**Fig. 4b**). In contrast to Dcr1, the dependency of Rdp1 binding on Clr4 differs between different genomic regions (**Figs. 3b**,**d** and **4b**). The association of Rdp1 with LTRs is independent of Clr4. Notably, those genomic features, such as LTRs, that show Clr4-independent Rdp1 binding are also those enriched in the Dcr1 DamID (**Fig. 4a**,**b**), suggesting that Rdp1 and Dcr1 may have a joint role in regulating these loci independently of heterochromatin. Indeed, transcripts originating from retrotransposon LTRs[31] were upregulated

Figure 4 Enrichment of Dam fusion proteins at different genomic features. (**a**–**c**) Dcr1, Rdp1 and Swi6 enrichments ($\log_2$) at the indicated genomic features in wild-type and heterochromatin-deficient (*clr4*Δ) cells. For all experiments, three biological replicates are shown. (**d**) ChIP experiment confirming physical association of Dcr1 with LTRs. The fold enrichment of Dcr1-TAP compared to a nontagged control, and normalized to actin and input, is shown. Error bars represent s.e.m. ($n = 3$). *P* value was generated using the Student's *t*-test; cendg, centromeric repeat element.

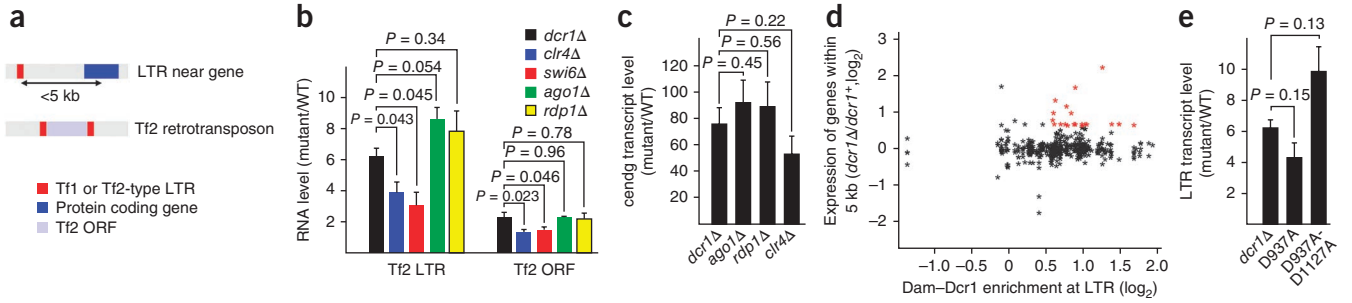

Figure 5 The *S. pombe* RNAi machinery contributes to LTR repression. (**a**) Schematic representation of LTRs and their position relative to protein coding genes (dark blue) or Tf2 retrotransposon ORFs (light blue). (**b**) Tf2 LTR and ORF transcript levels in the indicated mutant strains. (**c**) Dcr1, Ago1, Rdp1 and Clr4 are equally important for repression of centromeric repeats (cendg). (**d**) Genes within 5 kb of an LTR (measured from the middle of the gene to the middle of the LTR) were assessed for expression in Dcr1-deficient cells and for Dcr1 association with the nearby LTR. Genes whose expression was at least 1.5-fold increased in a *dcr1*Δ mutant and whose nearby LTR had at least 1.4-fold enrichment in the DamID data are highlighted in red and listed in **Supplementary Table 5**. (**e**) Tf2 LTR transcript levels in different *dcr1* mutants. D937A and D1127A are mutated sites in the RNaseIII catalytic centers of Dcr1. (**b**,**c**,**e**) RNA levels were normalized to actin and represented as fold increase compared to wild type. Error bars represent s.e.m., $n = 6$ biological replicates for *dcr1*Δ, $n = 3$ biological replicates for all other mutants. *P* values were generated using the Student's *t*-test.

in *dcr1Δ* and *rdp1Δ* cells (**Fig. 5a**,**b**). Similarly, LTR silencing was also affected in cells lacking the third fission yeast RNAi protein Ago1, implicating the *S. pombe* RNAi machinery in LTR repression (**Fig. 5b**). Notably, LTR derepression was significantly lower ($P = 0.043$ and $P = 0.045$, respectively) in *clr4*Δ or *swi6*Δ cells than in RNAi-deficient cells (**Fig. 5b**), suggesting that the conventional RNAi-mediated heterochromatin assembly pathway contributes only partly to their silencing. Consistent with this, Swi6 was not enriched at LTRs (**Fig. 4c** and data not shown). This is in contrast to the pattern for centromeric repeats, which are highly enriched for Swi6 and for which silencing is not significantly different ($P > 0.05$) between *clr4*Δ or RNAi-deficient cells (**Figs. 4c** and **5c**). Notably, silencing of Tf2 retrotransposon open reading frames (ORFs) was only slightly affected in RNAi and heterochromatin-deficient cells (**Fig. 5b**). Therefore, it seems likely that RNAi functions redundantly with other pathways to silence transposable elements in *S. pombe*[32,33].

Finally, it has previously been proposed that LTRs could regulate the expression of nearby genes in *S. pombe*, which led us to speculate that LTRs could function to create a local concentration of Dcr1, facilitating degradation of transcripts produced at nearby genes (**Fig. 5a**). However, comparing the enrichment of Dam–Dcr1 at LTRs with the expression of nearby genes in *dcr1*Δ cells did not reveal an overall positive correlation (**Fig. 5d**). Therefore, repression of nearby genes is unlikely to be a general feature of dispersed solo LTRs in *S. pombe*, although at this point we cannot rule out that some specific genes (**Supplementary Table 5**) are under direct control of LTRs and their associated RNAi proteins.

LTR silencing functions with trace amounts of siRNAs

A key feature of all RNAi-related pathways known to date is the presence of small RNAs that guide proteins of the Argonaute-Piwi family to their targets[34,35]. These mediate target RNA degradation, translational repression, or methylation of histone tails or DNA[36–38]. Therefore, the presence of siRNAs is a good criterion to define RNAi-mediated regulation. Because LTR silencing is dependent on all three *S. pombe* RNAi proteins (**Fig. 5b**), we expected to see substantial amounts of Dcr1-dependent siRNAs originating from Dcr1-associated LTRs and ncRNAs. However, we were not able to detect such siRNAs by northern blot techniques (data not shown). Even deep sequencing of total small RNAs or Ago1-bound small RNAs revealed only very few reads mapping to these sites (**Table 1**). Notably, although mutations in the RNase III domains of Dcr1, which abolish the processing of double-stranded RNAs into siRNAs, had the same effect on LTR silencing as deleting the *dcr1*$^+$ gene (**Fig. 5e**), only 29 out of 3×10^6 reads that map to the *S. pombe* genome could be uniquely assigned to LTRs (**Table 1**). These results demonstrate that siRNAs must be generated at LTRs, but that they are of extremely low abundance. Notably, these trace amounts of siRNAs seem to be sufficient to trigger a

Table 1 Small RNAs sequenced from wild-type and *dcr1Δ* cells

	Ago1-bound small RNAs				Total small RNAs			
	Wild type		*dcr1Δ*		Wild type		*dcr1Δ*	
	Reads	%	Reads	%	Reads	%	Reads	%
rRNA	1,705,697	56.72	4,883,712	91.57	52,742	55.51	226,615	69.97
tRNA	32,115	1.07	258,906	4.85	30,300	31.89	80,781	24.94
snRNA	728	0.02	5,669	0.11	418	0.44	1,798	0.56
snoRNA	650	0.02	1,994	0.04	283	0.30	909	0.28
3′ UTR	5,948	0.20	46,313	0.87	234	0.25	774	0.24
5′ UTR	2,982	0.10	1,998	0.04	129	0.14	164	0.05
mRNA	23,320	0.78	100,589	1.89	2,835	2.98	9,499	2.93
Intron	1,113	0.04	4,753	0.09	408	0.43	964	0.30
Centromeric	1,204,754	40.06	18,191	0.34	7,072	7.44	1,333	0.41
Mating type region	17,528	0.58	61	0.00	62	0.07	9	0.00
Replication origin	18	0.00	156	0.00	4	0.00	3	0.00
Pseudogene	1,247	0.04	138	0.00	23	0.02	25	0.01
LTR	29	0.00	471	0.01	11	0.01	22	0.01
wtf	19	0.00	154	0.00	152	0.16	70	0.02
ncRNA	11,296	0.38	10,078	0.19	341	0.36	915	0.28
Total	3,007,444	100	5,333,183	100	95,014	100	323,881	100

Weighted number of small RNA reads for different genomic features from deep sequencing of Ago1-bound small RNAs[19] or total small RNAs in wild-type and *dcr1Δ*. The number of reads for total small RNAs is lower, as barcoding was used to sequence several samples in one lane. snRNA, small nuclear RNA; snoRNA, small nucleolar RNA; UTR, untranslated region; wtf, with Tf2-type LTRs.

silencing response but function poorly in establishing a heterochromatic domain (**Figs. 4c** and **5b**,**e**). Similar to centromeric siRNAs in heterochromatin-deficient cells, the very low abundance of LTR siRNAs cannot be explained by the absence of the siRNA-processing machinery because both Rdp1 and Dcr1 are physically associated with LTRs (**Fig. 4a**,**b**). Therefore, we speculate that it may be Ago1 loading rather than siRNA biogenesis that depends on H3K9 methylation. We assume that unloaded siRNAs are prone to degradation, which would explain their low abundance in the absence of H3K9me.

DISCUSSION

In this study, we used DamID to probe the fission yeast genome for interactions with RNAi and heterochromatin proteins in a cell cycle–independent manner. Our findings provide new insights into the order of events during RNAi-mediated heterochromatin assembly and directly implicate RNAi proteins in repressing genomic elements other than the well-characterized centromeric repeats. Below, we discuss the implications of these findings for our understanding of nuclear RNAi.

RNAi-dependent Swi6 recruitment

The main function of the RNAi pathway in *S. pombe* was long thought to be assembly and maintenance of a heterochromatic structure at centromeric repeats. More recently, it has been demonstrated that RNAi also plays a key role in the transient recruitment of Swi6 to CGPs in the G1 phase or early S phase of the cell cycle[21]. Consistent with those results, we found Dcr1-dependent association of Swi6 with additional CGPs. However, on a genome-wide scale, Swi6 associates with only a few CGPs and shows no preference for association with CGPs when compared to other intergenic regions (data not shown), suggesting that Swi6 recruitment is unlikely to be a general or specific feature of CGPs in *S. pombe*.

Notably, our results revealed that there is a general agreement between the Dcr1-dependency of Swi6 binding to chromatin and association of such sites with Dcr1 itself. For example, Swi6 association with centromeres and ncRNAs requires Dcr1, and Dcr1 is associated with these regions. In contrast, Swi6 binding to the mating type region and telomeres is only partially dependent on Dcr1 (refs. 39,40), and Dcr1 does not associate with these regions. However, this does not apply for CGPs. Although Swi6 binding to CGPs is generally Dcr1-dependent, association of Dcr1 itself with these loci is not always observed (**Supplementary Table 2**), suggesting that RNAi does not necessarily need to act on chromatin to recruit Swi6 to CGPs. Consistent with this, RNAi proteins appeared to be largely excluded from CGPs on a genome-wide scale (**Supplementary Fig. 4**). We note that this does not rule out that the RNAi machinery may also function off chromatin to regulate the abundance of transcripts originating from CGPs on a truly post-transcriptional level[11] without recruiting Swi6, an intriguing possibility that deserves further study.

Heterochromatin-dependent accumulation of siRNAs

A remarkable observation in studies of RNAi in *S. pombe* is that the abundance of centromeric siRNAs depends on Clr4 or any of its associated proteins[7,14,15]. Unexpectedly, we found that Clr4 is dispensable for the association of Dcr1 and, partially, Rdp1 with centromeric repeats. These proteins were also found at euchromatic regions in the *S. pombe* genome, further demonstrating that H3K9 methylation is not a prerequisite for the association of the siRNA biogenesis machinery with chromatin. Based on these results, we favor a model in which efficient loading onto Ago1 rather than the biogenesis of siRNAs depends on H3K9me. We propose that Rdp1- and Dcr1-bound loci are poised for heterochromatin assembly, but that this is prevented by inefficient loading of Ago1 if H3K9 methylation is low or absent. If H3K9 methylation levels at such sites reach a certain threshold, this would then trigger a self-enforcing positive feedback mechanism in which siRNA-loaded RITS stably binds to the target locus via interactions with nascent RNA as well as methylated H3K9. This would lead to the recruitment of more Rdp1 and thereby activate siRNA amplification, eventually resulting in high levels of H3K9 methylation. This model predicts that alternative Clr4 recruitment mechanisms exist, which have yet to be identified. We note that ATF-CREB family proteins could serve this function at the mating type locus, where they have been shown to act in a parallel mechanism to the RNAi pathway to establish heterochromatin[39]. In summary, our data are consistent with a model in which some pre-existing H3K9 methylation is required for triggering an siRNA amplification loop, which is essential for efficient heterochromatin formation[8,36]. This may explain why siRNAs function poorly in *de novo* formation of heterochromatin *in trans*[5,11–13]. Notably, we provide evidence that Dcr1 and Rdp1 can function to degrade RNA in association with chromatin outside constitutive heterochromatin. This is consistent with a co-transcriptional gene silencing (CTGS) mechanism, as proposed earlier for heterochromatin silencing[5,22].

In contrast to yeast and plants, there is little evidence for a direct role of RNAi in gene silencing at the level of chromatin in other eukaryotes. Notably, this study demonstrates that even highly sensitive deep sequencing approaches may fail to identify all possible direct targets of the RNAi pathway. In addition, if CTGS were the only conserved function of RNAi in the nucleus of higher eukaryotes, attempts to find RNAi-dependent histone or DNA modifications in human cells could fail. Our results are opening up new avenues to address these issues, and we believe that approaches similar to those used in this study will disclose regions of other genomes that are under direct control of the RNAi pathway.

METHODS

Methods and any associated references are available in the online version of the paper at http://www.nature.com/nsmb/.

Accession codes. NCBI Gene Expression Omnibus: All datasets are deposited under accession number GSE24360.

Note: Supplementary information is available on the Nature Structural & Molecular Biology website.

ACKNOWLEDGMENTS

We thank H. Grosshans, A. Peters, F. Mohn and all members of the Bühler lab for critical comments on the manuscript; A.H. Brand for plasmids; B. van Steensel for advice; and H.-R. Hotz for bioinformatics support. We also thank the genomics facility of the Friedrich Miescher Institute for Biomedical Research for array hybridizations. This work was supported by the Swiss National Science Foundation and the Novartis Research Foundation.

AUTHOR CONTRIBUTIONS

K.J.W. and M.B. designed the research. K.J.W. designed and conducted experiments. D.G. wrote R scripts for data analysis. K.J.W. and D.G. analyzed the DamID data. T.P. conducted experiments. M.B. and K.J.W. analyzed the results and wrote the manuscript.

COMPETING FINANCIAL INTERESTS

The authors declare no competing financial interests.

Published online at http://www.nature.com/nsmb/.
Reprints and permissions information is available online at http://npg.nature.com/reprintsandpermissions/.

1. Volpe, T.A. *et al.* Regulation of heterochromatic silencing and histone H3 lysine-9 methylation by RNAi. *Science* **297**, 1833–1837 (2002).

2. Volpe, T. *et al.* RNA interference is required for normal centromere function in fission yeast. *Chromosome Res.* **11**, 137–146 (2003).
3. Reinhart, B.J. & Bartel, D.P. Small RNAs correspond to centromere heterochromatic repeats. *Science* **297**, 1831 (2002).
4. Verdel, A. *et al.* RNAi-mediated targeting of heterochromatin by the RITS complex. *Science* **303**, 672–676 (2004).
5. Bühler, M., Verdel, A. & Moazed, D. Tethering RITS to a nascent transcript initiates RNAi- and heterochromatin-dependent gene silencing. *Cell* **125**, 873–886 (2006).
6. Bayne, E.H. *et al.* Stc1: A critical link between RNAi and chromatin modification required for heterochromatin integrity. *Cell* **140**, 666–677 (2010).
7. Motamedi, M.R. *et al.* Two RNAi complexes, RITS and RDRC, physically interact and localize to noncoding centromeric RNAs. *Cell* **119**, 789–802 (2004).
8. Sugiyama, T., Cam, H., Verdel, A., Moazed, D. & Grewal, S.I. RNA-dependent RNA polymerase is an essential component of a self-enforcing loop coupling heterochromatin assembly to siRNA production. *Proc. Natl. Acad. Sci. USA* **102**, 152–157 (2005).
9. Cam, H.P. *et al.* Comprehensive analysis of heterochromatin- and RNAi-mediated epigenetic control of the fission yeast genome. *Nat. Genet.* **37**, 809–819 (2005).
10. Emmerth, S. *et al.* Nuclear retention of fission yeast dicer is a prerequisite for RNAi-mediated heterochromatin assembly. *Dev. Cell* **18**, 102–113 (2010).
11. Sigova, A., Rhind, N. & Zamore, P.D. A single Argonaute protein mediates both transcriptional and posttranscriptional silencing in *Schizosaccharomyces pombe*. *Genes Dev.* **18**, 2359–2367 (2004).
12. Iida, T., Nakayama, J. & Moazed, D. siRNA-mediated heterochromatin establishment requires HP1 and is associated with antisense transcription. *Mol. Cell* **31**, 178–189 (2008).
13. Simmer, F. *et al.* Hairpin RNA induces secondary small interfering RNA synthesis and silencing in trans in fission yeast. *EMBO Rep.* **11**, 112–118 (2010).
14. Noma, K. *et al.* RITS acts in cis to promote RNA interference-mediated transcriptional and post-transcriptional silencing. *Nat. Genet.* **36**, 1174–1180 (2004).
15. Hong, E.J., Villén, J., Gerace, E.L., Gygi, S.P. & Moazed, D. A cullin E3 ubiquitin ligase complex associates with Rik1 and the Clr4 histone H3–K9 methyltransferase and is required for RNAi-mediated heterochromatin formation. *RNA Biol.* **2**, 106–111 (2005).
16. Sadaie, M., Iida, T., Urano, T. & Nakayama, J. A chromodomain protein, Chp1, is required for the establishment of heterochromatin in fission yeast. *EMBO J.* **23**, 3825–3835 (2004).
17. Partridge, J.F. *et al.* Functional separation of the requirements for establishment and maintenance of centromeric heterochromatin. *Mol. Cell* **26**, 593–602 (2007).
18. Partridge, J.F. Centromeric chromatin in fission yeast. *Front. Biosci.* **13**, 3896–3905 (2008).
19. Halic, M. & Moazed, D. Dicer-independent primal RNAs trigger RNAi and heterochromatin formation. *Cell* **140**, 504–516 (2010).
20. Bühler, M. & Gasser, S.M. Silent chromatin at the middle and ends: lessons from yeasts. *EMBO J.* **28**, 2149–2161 (2009).
21. Gullerova, M. & Proudfoot, N.J. Cohesin complex promotes transcriptional termination between convergent genes in S. pombe. *Cell* **132**, 983–995 (2008).
22. Bühler, M. RNA turnover and chromatin-dependent gene silencing. *Chromosoma* **118**, 141–151 (2009).
23. Sadaie, M. *et al.* Balance between distinct HP1 proteins controls heterochromatin assembly in fission yeast. *Mol. Cell. Biol.* **23**, 6973–6988 (2008).
24. Bühler, M., Spies, N., Bartel, D.P. & Moazed, D. TRAMP-mediated RNA surveillance prevents spurious entry of RNAs into the *Schizosaccharomyces pombe* siRNA pathway. *Nat. Struct. Mol. Biol.* **15**, 1015–1023 (2008).
25. Djupedal, I. *et al.* Analysis of small RNA in fission yeast; centromeric siRNAs are potentially generated through a structured RNA. *EMBO J.* **28**, 3832–3844 (2009).
26. Buker, S.M. *et al.* Two different Argonaute complexes are required for siRNA generation and heterochromatin assembly in fission yeast. *Nat. Struct. Mol. Biol.* **14**, 200–207 (2007).
27. van Steensel, B. & Henikoff, S. Identification of *in vivo* DNA targets of chromatin proteins using tethered dam methyltransferase. *Nat. Biotechnol.* **18**, 424–428 (2000).
28. Bianchi-Frias, D. *et al.* Hairy transcriptional repression targets and cofactor recruitment in *Drosophila*. *PLoS Biol.* **2**, E178 (2004).
29. Bühler, M. & Moazed, D. Transcription and RNAi in heterochromatic gene silencing. *Nat. Struct. Mol. Biol.* **14**, 1041–1048 (2007).
30. Bowen, N.J., Jordan, I.K., Epstein, J.A., Wood, V. & Levin, H.L. Retrotransposons and their recognition of pol II promoters: a comprehensive survey of the transposable elements from the complete genome sequence of *Schizosaccharomyces pombe*. *Genome Res.* **13**, 1984–1997 (2003).
31. Mourier, T. & Willerslev, E. Large-scale transcriptome data reveals transcriptional activity of fission yeast LTR retrotransposons. *BMC Genomics* **11**, 167 (2010).
32. Cam, H.P., Noma, K., Ebina, H., Levin, H.L. & Grewal, S.I. Host genome surveillance for retrotransposons by transposon-derived proteins. *Nature* **451**, 431–436 (2008).
33. Anderson, H.E. *et al.* The fission yeast HIRA histone chaperone is required for promoter silencing and the suppression of cryptic antisense transcripts. *Mol. Cell. Biol.* **18**, 5158–5167 (2009).
34. Peters, L. & Meister, G. Argonaute proteins: mediators of RNA silencing. *Mol. Cell* **26**, 611–623 (2007).
35. Ghildiyal, M. & Zamore, P.D. Small silencing RNAs: an expanding universe. *Nat. Rev. Genet.* **10**, 94–108 (2009).
36. Moazed, D. Small RNAs in transcriptional gene silencing and genome defence. *Nature* **457**, 413–420 (2009).
37. Law, J.A. & Jacobsen, S.E. Establishing, maintaining and modifying DNA methylation patterns in plants and animals. *Nat. Rev. Genet.* **11**, 204–220 (2010).
38. Chapman, E.J. & Carrington, J.C. Specialization and evolution of endogenous small RNA pathways. *Nat. Rev. Genet.* **8**, 884–896 (2007).
39. Jia, S., Noma, K. & Grewal, S.I. RNAi-independent heterochromatin nucleation by the stress-activated ATF/CREB family proteins. *Science* **304**, 1971–1976 (2004).
40. Kanoh, J., Sadaie, M., Urano, T. & Ishikawa, F. Telomere binding protein Taz1 establishes Swi6 heterochromatin independently of RNAi at telomeres. *Curr. Biol.* **15**, 1808–1819 (2005).

ONLINE METHODS

Strains and plasmids. Fission yeast strains (grown at 30 °C in YES medium, MP Biomedicals no. 4101-532) and plasmids used in this study are described in **Supplementary Tables 6** and **7**. All strains were constructed following a standard PCR-based protocol[41] or by random spore analysis. DamMyc was cloned from pNDamMyc using XhoI and AscI into expression vectors pJR-L-3x or pJR-L-81x for high or low expression of the fusion, respectively[42]. For expression of unfused Dam, a stop codon was introduced after the Myc sequence. The protein of interest was inserted at the C terminus of DamMyc using ApaI and SmaI restriction sites. For PCR-based insertion of the fusion protein into the yeast genome, the whole sequence, including nmt1(81×) promoter and terminator, was cloned into plasmid pFA6a-kanMX6 (ref. 41) using In-Fusion PCR Cloning (Clontech) with PacI and BglII sites. This plasmid was used for PCR-based insertion of the construct into the *leu1* locus. Primer sequences used for cloning are available upon request. Constructs on plasmids and in yeast strains were confirmed by sequencing.

DamID. Strains expressing either unfused Dam or Dam fusion proteins were grown to OD_{600} = 0.4. Approximately 5.3×10^7 cells were harvested, washed once with water and flash frozen in liquid nitrogen. Cells were spheroplasted in 500 µl spheroplast buffer (1.2 M sorbitol, 100 mM $KHPO_4$, pH 7.5, 0.5 mg ml^{-1} Zymolyase (Zymo Research), 1 mg ml^{-1} lysing enzyme from *Trichoderma harzianum* (Sigma)). Genomic DNA was isolated using the DNeasy Blood and Tissue Kit (Qiagen). The DamID protocol was carried out as previously described[43], except that dUTP was included in the PCR reaction to allow fragmentation and labeling using the GeneChip Whole Transcript Double-Stranded DNA Terminal Labeling Kit (Affymetrix). The fragmented and labeled DNA was hybridized to GeneChip *S. pombe* Tiling 1.0FR Arrays (Affymetrix).

RNA isolation, cDNA synthesis and quantitative RT-PCR. Done as described previously[10]. Primer pairs used for PCR reactions can be found in **Supplementary Table 8**.

Statistical analysis. All *P* values were generated using the Student's *t*-test (two-tailed distribution, two-sample unequal variance). All error bars show the s.e.m., where *n* is at least three independent biological replicates.

Chromatin immunoprecipitation and northern blotting. Dcr1-TAP ChIP was done as described[5] except that cross-linking was done with 3% fresh formaldehyde. Sheep anti-mouse IgG Dynabeads (Invitrogen) were used. Centromeric siRNAs were isolated and detected by northern blotting as described previously[5].

Expression profiling. Previously published datasets were used for expression analysis of *dcr1Δ* cells[10].

Normalization of the tiling array data from DamID experiments. All tiling arrays were processed in R[44,45], using bioconductor[46] and the packages tilingArray[47] and preprocessCore. The arrays were RMA background corrected, quantile normalized and $\log_2$ transformed on the oligo level, using the following command: expr <- log2(normalize.quantiles(rma.background.correct(exprs(read Cel2eSet(filenames,rotated = TRUE))))). Contrasts were computed on the oligo level by subtracting respective columns of expression.

Reannotation of the Affymetrix *S. pombe* Tiling 1.0FR Array. The sequences of the 1174792 perfect-match oligos were extracted from the BPMAP file Sp20b_M_v04.bpmap (http://www.affymetrix.com/estore/browse/products.jsp?navMode=34000&productId=131500&navAction=jump&aId=productsNav#1_3) using the readBpmap function from the affxparser package. Alignment to the *S. pombe* genome (8 May 2009, http://www.sanger.ac.uk/Projects/S_pombe/) was done by using the software bowtie (version 0.9.9.1)[48], allowing for up to 100 matches per oligo.

Correcting a bias caused by variable fragment size between GATC restriction sites. While inspecting oligo level contrasts in a genome browser, we noticed enrichment breakpoints coinciding with GATC restriction sites (**Supplementary Fig. 1c**). We therefore speculated that during sample preparation, certain fragment sizes might be depleted or enriched. Plotting the fragment sizes between two GATC restriction sites against the average enrichment in the corresponding fragment confirmed this observation on a genome-wide scale (**Supplementary Fig. 1d**). We speculated that this resulted from small differences in the sample preparation process, probably during the step of size selection. In addition to fragment size–dependent mean enrichment or depletion, we noticed discontinuity of the contrast variability coinciding with GATC restriction sites. We plotted the fragment sizes between two GATC restriction sites against the s.d. of the enrichment in the corresponding fragment and observed discontinuities on a genome-wide level (**Supplementary Fig. 1d**). Both observed effects are highly unlikely to be of biological origin because they are tightly correlated to the fragment size between GATC restriction sites. Therefore, we designed software that would at least partially reverse the bias and correct the initial data. For every contrast independently, the corrector walks through all the fragments (between GATCs) and adjusts the mean and the s.d. of all the oligos that are located within the fragment. The adjustment is dependent on fragment size, and the extent of correction is determined from the lowess fit of the corresponding contrast. In more detail, for a given fragment size, the value of the lowess smoother is evaluated and compared to the average level of the given contrast. The corrector therefore does not modulate the overall mean or the variability of the contrasts. **Supplementary Figure 1c** shows the result of the corrector for one genomic locus.

***S. pombe* genome annotation.** The *S. pombe* annotation file pombe_160708.gff was downloaded from http://www.sanger.ac.uk/Projects/S_pombe/ and used to compile annotation categories for rRNA, tRNA, snRNA, snoRNA, 3′ UTR, 5′ UTR, mRNA, intron, centromeric, telomeric, mating type region, replication origin, pseudogene, LTR, wtf ('with Tf2-type LTRs') and ncRNA. Intergenic regions were generated from the mRNA annotation, not considering any regions interrupted by rRNA, tRNA, centromeric, snRNA, snoRNA and mating type region. Using the tiling arrays, we computed (differential) expression values for either individual features (for example, a transcript) or whole annotation categories by averaging enrichment values for all the oligos overlapping the respective regions. In the case of individual feature quantification, we considered only features covered by at least 50 oligos.

Reannotation of various publicly available datasets. Publicly available datasets[9,10,19] were downloaded and remapped to the *S. pombe* genome (8 May 2009) and reannotated based on the categories described above.

Deep sequencing. For Ago1-bound small RNAs, previously published data were downloaded and reannotated as above[19]. For total small RNAs, sample libraries were prepared and analyzed as previously described[10].

41. Bähler, J. *et al.* Heterologous modules for efficient and versatile PCR-based gene targeting in *Schizosaccharomyces pombe*. *Yeast* **14**, 943–951 (1998).
42. Moreno, M.B., Duran, A. & Ribas, J.C. A family of multifunctional thiamine-repressible expression vectors for fission yeast. *Yeast* **16**, 861–872 (2000).
43. Vogel, M.J., Peric-Hupkes, D. & van Steensel, B. Detection of *in vivo* protein-DNA interactions using DamID in mammalian cells. *Nat. Protoc.* **2**, 1467–1478 (2007).
44. The R Development Core Team. R: A language and environment for statistical computing. ⟨http://cran.r-project.org⟩ (2004).
45. Ihaka, R. & Gentleman, R.R. A language for data analysis and graphics. *J. Comput. Graph. Statist.* **5**, 299–314 (1996).
46. Gentleman, R.C. *et al.* Bioconductor: open software development for computational biology and bioinformatics. *Genome Biol.* **5**, R80 (2004).
47. Huber, W., Toedling, J. & Steinmetz, L.M. Transcript mapping with high-density oligonucleotide tiling arrays. *Bioinformatics* **22**, 1963–1970 (2006).
48. Langmead, B., Trapnell, C., Pop, M. & Salzberg, S.L. Ultrafast and memory-efficient alignment of short DNA sequences to the human genome. *Genome Biol.* **10**, R25 (2009).

doi:10.1038/nsmb.1935